Journal of Alloys and Compounds 506 (2010) 520–525

Contents lists available at ScienceDirect

Journal of Alloys and Compounds

journal homepage: www.elsevier.com/locate/jallcom

Surface oxidation and magnetic properties of $(Cu_{60}Co_{40})_{68}Zr_{32}$ glassy ribbons

B. Schwarz[a,*], N. Mattern[a], S. Oswald[a], J. Eckert[a,b]

[a] Leibniz-Institute IFW Dresden, Institute for Complex Materials, P.O. Box 270116, Helmholtz-strasse 20, D-01171 Dresden, Germany
[b] TU Dresden, Institute of Materials Science, D-01062 Dresden, Germany

ARTICLE INFO

Article history:
Received 10 May 2010
Received in revised form 7 July 2010
Accepted 9 July 2010
Available online 16 July 2010

Keywords:
Metallic glasses
Oxidation
DSC
XRD
SEM
EDX
XPS

ABSTRACT

The evolution of local Co density during thermal annealing of $(Cu_{60}Co_{40})_{68}Zr_{32}$ glassy ribbons was intended to be probed by in situ and ex situ magnetization measurements. However, even when the as-quenched sample is exposed to air at room temperature for several hours, Zr becomes strongly enriched at the surface due to selective oxidation and material in the adjacent sample volume subsequently separates into Co-rich and Cu-rich phases and the magnetic properties are decisively affected by these processes taking place within the first 20 nm from the surface. In this paper we report on the characterization of the oxidation and separation processes at the $(Cu_{60}Co_{40})_{68}Zr_{32}$ glassy ribbons' surface by means of differential scanning calorimetry (DSC), X-ray diffraction (XRD), scanning electron microscopy (SEM), energy dispersive X-ray spectroscopy (EDX), magnetization measurements and X-ray photoelectron spectroscopy (XPS) and point out why the results of magnetization measurements, especially for this type of materials, i.e. metallic ribbons with a high ratio of surface to volume, have to be considered critically in general.

1. Introduction

Cu–Zr [1–3] as well as Co–Zr [3–6] binary alloy systems are well known for their good glass forming ability in a wide compositional range. In this work ternary $Cu_{41}Co_{27}Zr_{32}$ glassy ribbons were prepared by rapid quenching techniques. Especially, since Cu and Co have a positive enthalpy of mixing and the binary Cu–Co system exhibits a metastable liquid–liquid as well as a stable solid–solid miscibility gap [7–10], peculiar amorphous–amorphous phase separation into Cu- and Co-rich phases or cluster formation prior to crystallization were assumed to be likely to occur during thermal annealing well below the crystallization temperature as determined from DSC measurements. Since elemental Zr and Cu are weak paramagnetic and diamagnetic, respectively, especially the potential increase of the local Co density accompanied by an increase of the number of Co as next neighbors of a central Co atom induced by the annealing, will lead to enhanced paramagnetism or even to ferromagnetism regardless whether the phases are crystalline or amorphous. Monitoring the changes of magnetic properties during the annealing process was thought to represent an appropriate way to get more insight into chemical and/or structural changes in the bulk material. However, we will demonstrate in this study that surface oxidation and subsequent phase separation processes in regions close to the surface will decisively affect the experimental results.

2. Experimental

Pre-alloyed ingots with nominal composition $(Cu_{60}Co_{40})_{68}Zr_{32}$ were prepared by arc-melting elemental Cu, Co and Zr with purities of 99.9 at.% or higher in a Ti-gettered argon atmosphere. To ensure homogeneity, the samples were remelted several times. From the pre-alloys thin ribbons (5 mm width and 30–40 μm in thickness) were prepared by single roller melt spinning under argon atmosphere. XRD patterns were recorded in transmission geometry with Mo Kα radiation using a STOE STADI P diffractometer. The structure was further analyzed by TEM using a JEOL JEM 2100F device and the ribbons were thinned by ion beam sputtering using a Gatan Inc. PIPS 691 with cold stage. The thermal behavior was investigated by DSC with a Perkin-Elmer DSC 7 in argon 5.0 atmosphere. The microstructure was analyzed by scanning electron microscopy (SEM) using a Gemini device (Zeiss) with EDX detector. Measurements of magnetization as a function of temperature up to 800 K was performed with a Superconducting Quantum Interference Device (SQUID) from Quantum Design equipped with a high temperature oven option. The sample was mounted in an open quartz ampulla in the standard low pressure He atmosphere. XP spectra were measured on a PHI 5600 CI system using an Al Kα 350 W monochromatized X-ray source and a hemispherical analyzer. Sputter depth profiling was performed using 3.5 keV Ar^+ ions at conditions leading to a sputtering rate of approximately 1 nm/min. Concentration quantification was done using single-element standard sensitivity factors assuming a homogeneous mixture of the elements in the information depth region.

3. Results and discussion

The diffuse character of the scattering curve shown in Fig. 1a indicates the amorphous state of the as-quenched sample that was unambiguously confirmed by high resolution transmission

* Corresponding author. Tel.: +49 0351 4659 846; fax: +49 0 351 4659 452.
E-mail address: b.schwarz@ifw-dresden.de (B. Schwarz).

0925-8388/$ – see front matter © 2010 Elsevier B.V. All rights reserved.
doi:10.1016/j.jallcom.2010.07.079

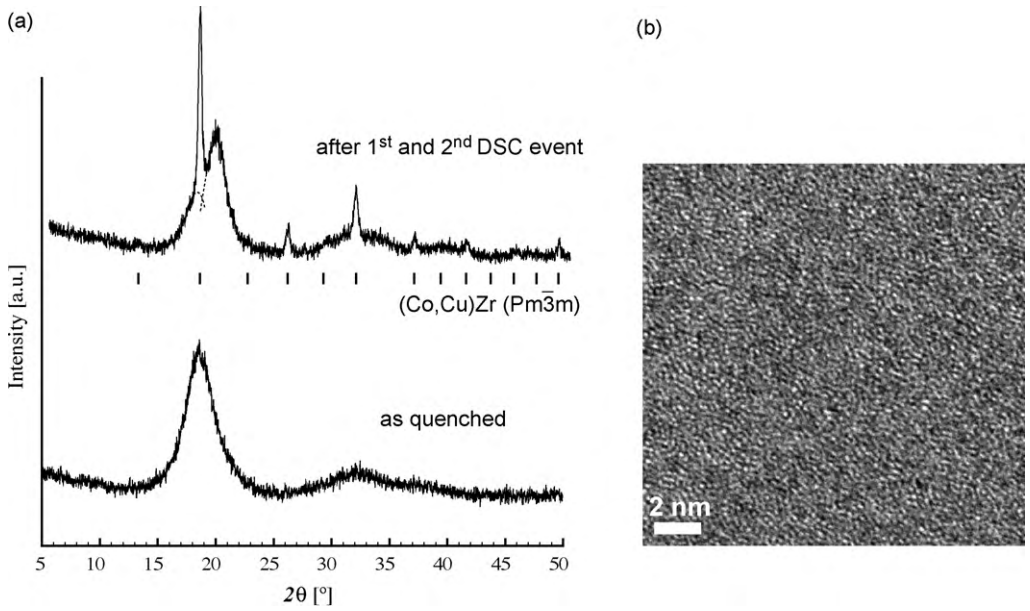

Fig. 1. (a) Powder diffraction patterns of $(Cu_{60}Co_{40})_{63}Zr_{37}$ samples in the as-quenched state and after heating slightly above the first and second DSC event. The vertical ticks show the calculated positions of the Bragg reflections of the B2 (Co,Cu)Zr [12,13] structure ($Pm\bar{3}m$). (b) High resolution transmission electron microscopy image of an amorphous $(Cu_{60}Co_{40})_{63}Zr_{37}$ sample in the as-cast state.

electron microscopy investigations (Fig. 1b). The DSC traces for a variety of heating rates for $(Cu_{60}Co_{40})_{68}Zr_{32}$ glassy ribbons are presented in Fig. 2. The temperatures of the first and second exothermic event, defined as peak value at 10 K/min, are 764(2) K and 775(2) K, respectively. After heating to 823 K, i.e. slightly above the first and second DSC event, at a rate of 60 K/min in flowing argon atmosphere and subsequently free cool down to room temperature, a crystalline cubic phase with (Co,Cu)Zr [12,13] structure ($Pm\bar{3}m$, $a_0 = 3.199(1)$ Å) has formed (see Fig. 1). By applying Vegard's law [14] it can be deduced from the lattice parameter, determined by Rietveld refinement [15], that it is essentially the CoZr phase with only minor incorporation of Cu (a_0(CoZr) = 3.197(1) Å; a_0(CuZr) = 3.262(1) Å). Furthermore, a diffuse halo with increased maximum position in q-space and slightly lowered full width at half maximum still exists. Due to the precipitation of the CoZr phase that has a higher Zr content than the initial amorphous $(Cu_{60}Co_{40})_{68}Zr_{32}$ phase the remaining material is Zr depleted and, since Cu (135(5)pm) and Co (135(5)pm) have approximately the same atomic radius, but that of Zr (155(5)pm) is comparably larger [11], its diffuse maximum is shifted to higher q values. The lowered full width at half maximum of this broad reflection indicates that this Zr depleted phase is at least partially nano crystalline and not fully amorphous any more. This is further confirmed by more detailed investigations of samples that were annealed at higher temperatures and/or for longer periods of time. The dashed lines indicate that the halo actually consists of two diffuse reflections hardly conceivable due to the simultaneous presence of the crystalline reflection at this q range. Magnetization as a function of temperature, measured in situ at a constant magnetic field of $\mu_0 H = 5$ T, is depicted in Fig. 3. The temperature was increased from 300 K to 800 K with a heating rate of 10 K/min, isothermally held at 800 K for 40 min, and decreased from 800 K to 550 K with a rate of −10 K/min and from 550 K on the temperature approached more slowly 300 K again. Starting with 0.11(1) A m^2 kg^{-1} at 300 K the magnetization remains nearly constant at this value up to 580 K. During the ongoing temperature increase the magnetization steeply increases, passes through

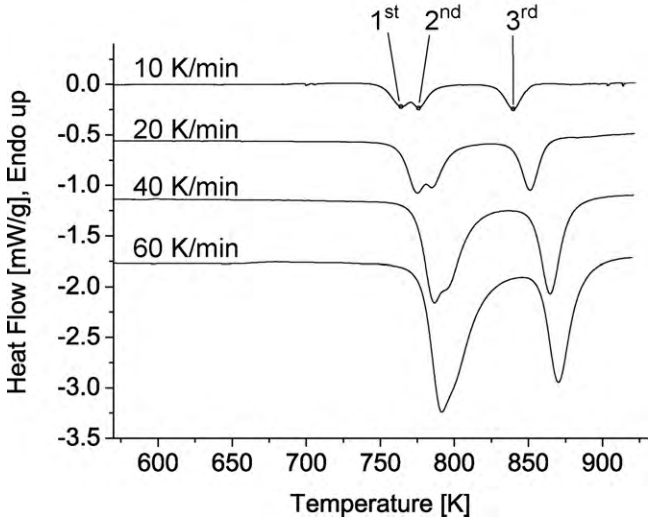

Fig. 2. DSC traces for various heating rates of $(Cu_{60}Co_{40})_{68}Zr_{32}$ metallic glasses prepared by melt spinning.

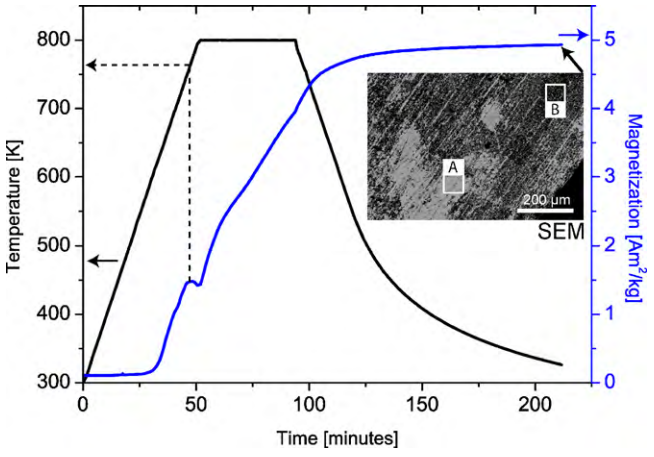

Fig. 3. In situ measurement of magnetization vs. temperature of a $(Cu_{60}Co_{40})_{68}Zr_{32}$ glassy ribbon at a constant magnetic field of $\mu_0 H = 5$ T.

a local minimum at ≈760 K and approaches a constant value of about to 4.9 A m^2 kg^{-1} shortly after the temperature decreases again. In the XRD pattern a very weak reflection at $q = 2.19$ Å^{-1} can be observed after the annealing, indicating that small amounts of ZrO_2 [17] (P42/nmc) phase has been formed. The inset in Fig. 3 presents a SEM image with back scattering electron contrast of the sample's surface after the in situ annealing. EDX analyses at the bright (A) and dark (B) phase reveal the nominal compositions of $O_{45(2)}Zr_{28(2)}Co_{14(2)}Cu_{13(2)}$ and $Cu_{47(2)}O_{21(2)}Co_{12(2)}Zr_{10(2)}$, respectively. Since the information depth with EDX is in the μm range and the different layers are considerably thinner, these results are falsified to a certain extend and do not reflect the actual composition of the different phases. Taking into account the results from XPS measurements (see below), the dark phase (B) is predominantly ascribed to metallic Cu that segregated to the surface after ZrO_2 (bright phase A) has formed at the surface. Grinding off several μm of material from the samples' surfaces reduces the mass specific magnetization dramatically and it approaches the value of the as-quenched material again. This clearly indicates that the changes of magnetization during the in situ annealing in low pressure He atmosphere is totally dominated by processes occurring at the samples' surface. As will be revealed in the following in more detail at first ZrO_2 is formed at the surface of the material and during an ongoing thermal treatment Cu finally segregates to the surface, so that in the case of a long term annealing in oxidizing environment only the Cu- and Zr-rich phases on the top are detectable with EDX analyses and the Co-rich phases, mainly contributing to the magnetic properties, are located beneath and are not accessible. The local minimum in the in situ magnetization annealing experiment at ≈760 K relates to the inherent bulk crystallization processes that reduce the paramagnetic susceptibility. That means that there is a considerable reduction of the paramagnetic susceptibility when Co that was formerly incorporated in the amorphous Cu–Co–Zr matrix forms the crystalline CoZr phase.

Since the oxidation/separation processes at the surface still continue there is an overall trend for increasing magnetization and the crystallization event of the bulk material is only represented by a local minimum. Comparable strong effects of oxidation/separation on the magnetic properties were also obtained when the sample was annealed ex situ in a DSC device under flowing argon 5.0, specified to contain less than 2 ppm oxygen. From these results we conclude that neither the He gas at low pressure, that is standardly present in the sample chamber for SQUID operations, nor argon 5.0 are appropriate for annealing experiments of this kind of material, since the small oxygen contaminations are sufficient to decisively modify the samples' surfaces and potential small changes of bulk magnetic properties are totally obscured by these processes. Therefore, we investigated to what extend the surfaces of $(Cu_{60}Co_{40})_{68}Zr_{32}$ glassy ribbons are already modified when annealed at very moderate conditions by XPS and magnetization measurements. Fig. 4 presents the depth profiles of elemental composition determined by XPS for (a) an as-quenched sample with ground off surface, (b) an as-quenched sample which surface was ground off and exposed to air several hours at room temperature and (c) an annealed sample at a moderate temperature of 573 K for only 30 min in vacuum (<10^{-4} mbar). In order to illustrate the drastic change of oxygen concentration from the surface towards the bulk on the one hand and the depth profile of only metallic components on the other hand clearly in a single graph, the concentrations of the metallic elements were determined without considering the oxygen, i.e. $x_{Co} + x_{Cu} + x_{Zr} = x_{met} = 100\,\%$ and $x_O + x_{met} = 100\,\%$. Even the sample that was ground off immediately before investigation is oxidized within the first 15 nm from the surface (Fig. 4a). In this region Zr is enriched and Co and Cu are depleted, Cu exhibiting a maximum between 10 nm and 15 nm at the position where Zr reached its bulk concentration again. The as-quenched sample

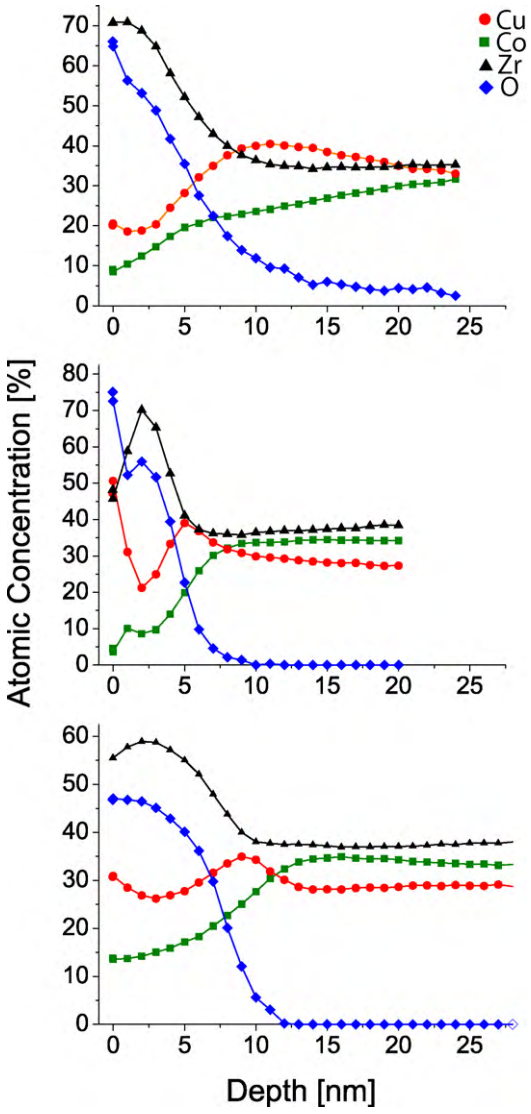

Fig. 4. Elemental concentrations versus sample depth obtained by XPS combined with ion sputtering for $(Cu_{60}Co_{40})_{68}Zr_{32}$ samples prepared by melt spinning: (a) as quenched with sandpapered surface immediately before investigation; (b) as quenched several hours exposed to air at room temperature; (c) Sample annealed at 573 K for 30 min in vacuum <10^{-4} mbar.

without ground off surface, i.e. exposed to air for several hours, shows a high oxygen content within the first 10 nm (Fig. 4b). Again, Zr is enriched in this region, but Cu has two maxima, one directly at the surface and another approximately at the position where Zr reaches its bulk concentration again. Co reaches its bulk concentration within a shorter distance from the surface. Nearly the same situation is present for a sample that was annealed isothermally at 573 K for 30 min with the difference that here even a maximum in the Co concentration slightly below the Cu maximum is observable (Fig. 4c). From a detailed investigation of the peak shape and position, the depth dependent element specific oxidation state was determined additionally. Cu as well as Co are metallic over the whole measuring range and only Zr is oxidized at the surface. Fig. 5 shows the accompanied shift of the Zr $3d_{5/2}$ and $3d_{3/2}$ peak doublet from higher to lower binding energies when Zr changes its state from oxidic to metallic in dependence of the sample depth [16]. Overall, it can be deduced that due to selective oxidation Zr segregates to the surface if the sample environment is not completely free of oxygen. However, an associated

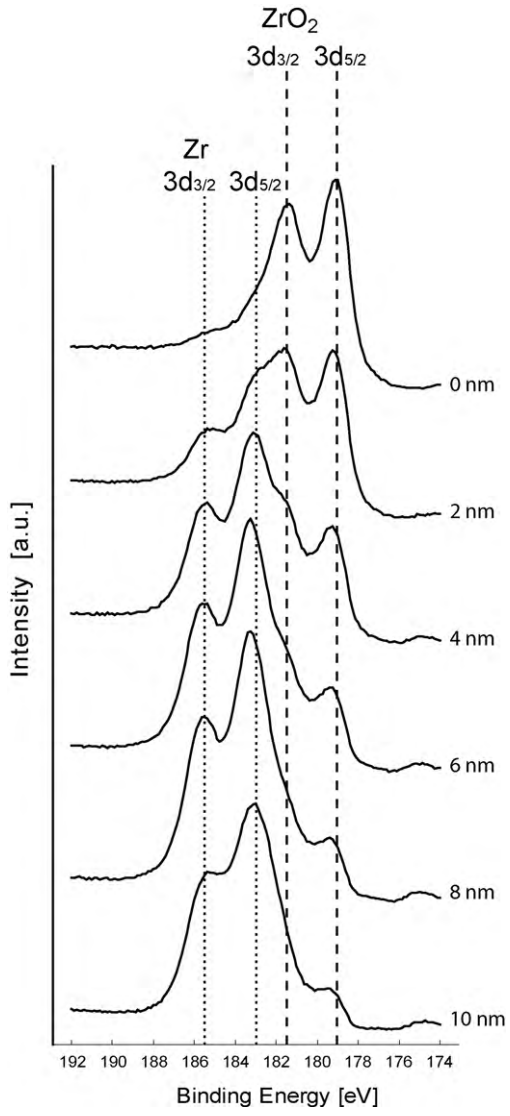

Fig. 5. Section of a XPS spectrum showing the Zr 3*d* peaks as a function of sample depth for a $(Cu_{60}Co_{40})_{68}Zr_{32}$ glassy ribbon annealed at 573 K for 30 min in vacuum $<10^{-4}$ mbar. The dashed and dotted lines indicate the binding energies for the $3d_{5/2}$ and $3d_{3/2}$ peak of metallic Zr and ZrO_2, respectively [16].

Zr depletion in adjacent sample regions is only indicated to a minor extend. This is followed by a subsequent Cu enrichment at the outer surface as well as at the interface where Zr changes from being oxidic to metallic. A phase separation into Cu- and Co-rich phases is clearly indicated for the sample annealed at 573 K by the formation of a Cu and a Co concentration maximum at about 8 nm and 15 nm, respectively. XPS is very sensitive concerning the detection of oxygen and these investigations give evidence that during production of the metallic glass by melt spinning in argon atmosphere there is no noticeable oxide contamination of the bulk material. On the other hand they demonstrate that the surface is modified considerably already at rather moderate conditions. The samples (a)–(c) were also characterized magnetically by measuring hysteresis loops at various temperatures from 5 K to 300 K (Fig. 6). Above 50 K all samples show temperature independent pauli paramagnetism with linear dependence of magnetization M on the field up to $\mu_0 H = 7$ T that is ascribed mainly to the bulk material. Additionally, a certain small part of sample (a) and (b) exhibits ferro/ferrimagnetism with remanent magnetization up to room temperature and coercivity at very low temperature, exemplarily shown for 5 K. Contrary, sample (c), annealed isothermally at 573 K for 30 min, shows a very strong increase of magnetization of one order of magnitude due to ferro/ferrimagnetic ordering at low temperature. From temperature scans at low fields the ordering temperature can be determined to be below 20 K. A certain coercivity that is existent from 300 K on vanishes at very low temperature when the magnetic ordering sets in. Although the magnetic susceptibilities obtained from ground off samples at high fields, i.e. ferro-/ferrimagnetic parts should not contribute due to saturation, are of the same order of magnitude ($0.90 < \chi\ [10^{-9}\ m^3\ mol^{-1}] < 2.05$) as comparable metallic glasses $Co_{25}Zr_{75}$ ($\chi = 2.110^{-9}\ m^3\ mol^{-1}$) [18] and $Cu_{41}Zr_{59}$ ($\chi = 1.410^{-9}\ m^3\ mol^{-1}$) [19], it is not clear to which extend regions near to the modified surface contribute to the signal. We propose the following model to explain the dependence of magnetic properties on the sample state: Induced by the oxidation of Zr at the surface, material near to the surface is assumed to separate into Co- and Cu-rich phases. During the initial stages of separation as present in sample state (a) and (b) small amounts of Co-rich Co–Cu–Zr phases with a certain coercivity are formed in the direct vicinity of the ZrO_2 layer and are responsible for the partial weak ferromagnetic contribution. During the annealing at 573 K for 30 min the separation in Co- and Cu-rich regions continuous. The fact that the magnetic ordering with strong increase of magnetization sets in at very low temperature of about 20 K indicates that only weak exchange interactions between magnetic centers are present and we suggest a weak RKKY-like magnetic coupling between the Co-rich regions mediated via the Cu-rich regions. Below 20 K the coercivity of the individual Co-rich regions is averaged out by the ferromagnetic coupling between the individual Co-rich particles and the regions near to samples surface now act like a soft ferromagnet with corresponding large increase of saturation magnetization. Within the framework of this assumption the soft magnetic behavior seems to be reasonable despite the fact that even Co–Zr alloys with Zr contents below 20 at.% normally exhibit considerable coercivities [20,21]. The presence of large amounts of pure Co that is also known to be soft magnetic on the other hand seems to be unreasonable from a phase constitutional point of view and furthermore magnetic order would already set in above room temperature. Table 1 shows the molar susceptibilities χ_m for elemental Cu, Co, Zr and for various crystalline Cu–Zr and Co–Zr compounds [19,18]. In the first place the number of next nearest Co atoms and their distance

Table 1
Molar susceptibilities χ_m for elemental Cu, Co, Zr and for various crystalline Cu–Zr and Co–Zr compounds [19,18].

Co–Zr compound	χ_m [10^{-9} m^3 mol^{-1}]	Cu–Zr compound	χ_m [10^{-9} m^3 mol^{-1}]
Zr	1.722	Zr	1.722
$CoZr_3$	2.061		
$CoZr_2$	2.212	$CuZr_2$	0.616
CoZr	4.335	$Cu_{10}Zr_7$	1.131
Co_2Zr	5.429	Cu_3Zr	0.490
$Co_{23}Zr_6$	ferro.		
$Co_{11}Zr_2$	ferro.		
Co	ferro.	Cu	−0.068

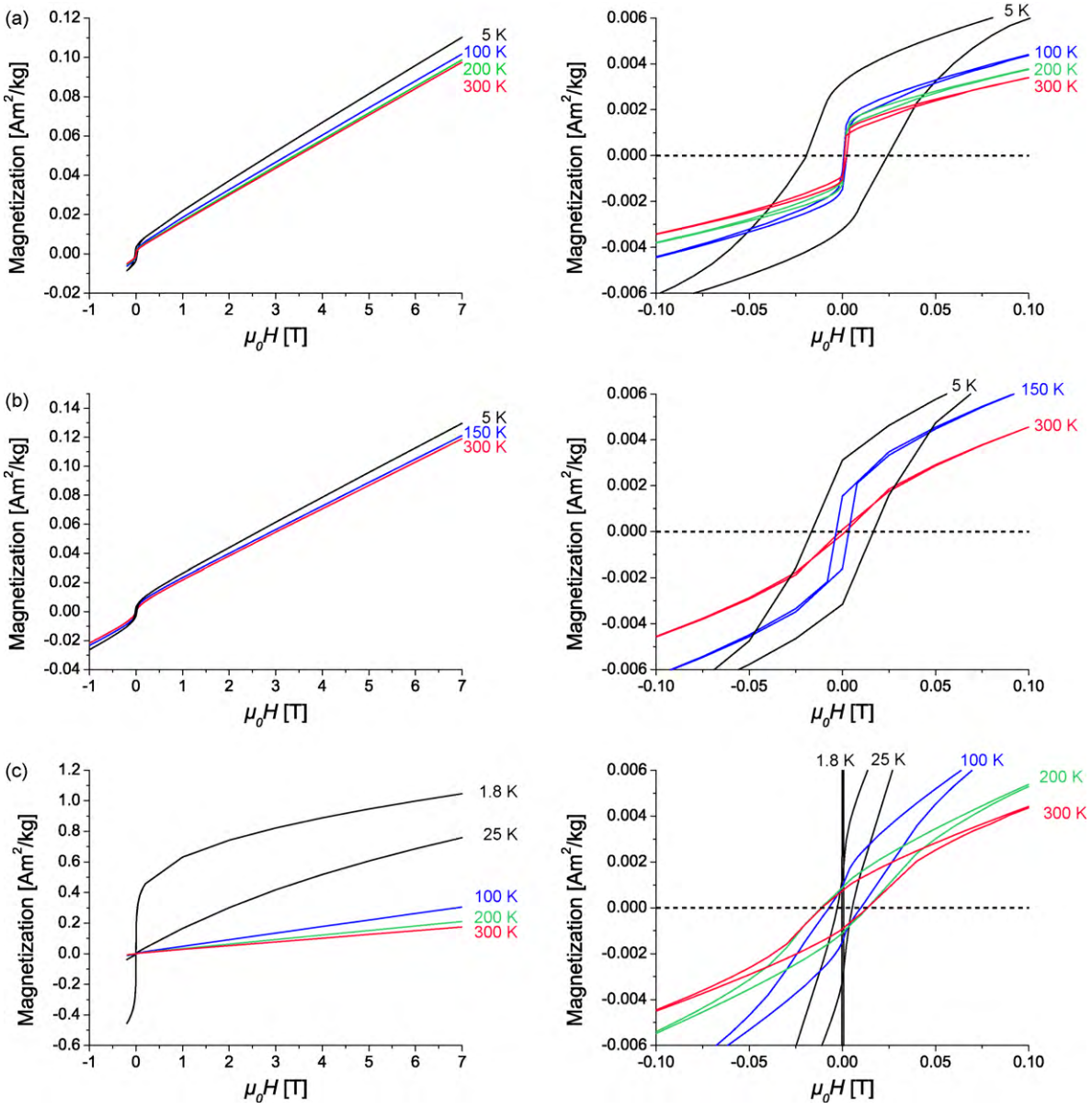

Fig. 6. Magnetization vs. magnetic field for various temperatures of $(Cu_{60}Co_{40})_{68}Zr_{32}$ samples prepared by melt spinning. On the right hand side an enlarged section at the vicinity of the origin is shown. (a) Representative for all samples (as quenched as well as heat treated) with ground off surface, (b) as quenched and several hours at air, (c) sample held at 573 K for 30 min in vacuum $<10^{-4}$ mbar.

to a central Co atom determine, whether the compound orders ferromagnetically or not so that the given information also serves as a criterion for which minimum Co content ferromagnetism should also be expected for amorphous compositions. Since ferromagnetism is predicted for Co contents exceeding 80 at.% in $Co_{23}Zr_6$, but it is at maximum 35 at.% determined for the sample annealed isothermally at 573 K for 30 min, a decomposition in more Co-rich phases on a length scale that is practically not resolvable with the XPS depth profiling is possible. In [22] the formation of a Zr-rich surface during the thermal annealing of a $Cu_{30}Zr_{70}$ glassy ribbon is ascribed to the selective oxidation and to lattice strain during the annealing treatment. Lu et al. state that if the sample environment would not be completely free of oxygen, the element Zr would be oxidized and became enriched on the surface, whereas the remaining atoms of elemental Cu would cluster and precipitate in a sub-surface layer. We interpret this as the initial state of the annealing and found that Cu will finally also be enriched at the surface during an ongoing annealing.

4. Conclusions

Due to the oxidation and subsequent separation processes at regions near to the surface observed for $(Cu_{60}Co_{40})_{68}Zr_{32}$ glassy ribbons, potential small changes of the weak bulk magnetism due to structural/chemical redistributions are totally obscured and magnetization measurements are not an appropriate method to probe structural changes in this case, since it is practically not possible to completely remove the glassy ribbons' surface material due to pronounced roughness and even presence of pores. Even the sample that is ground off directly before the XPS analysis exhibits a modified surface due to oxidation and segregation processes that occurred during a short period of time at room temperature and consequently also the magnetic properties are modified showing hysteresis effects at low temperature despite the fact that the bulk sample still is supposed to be paramagnetic. This work exemplarily shows that the results of magnetization measurements, especially for this type of materials, i.e. metallic ribbons with a high ratio of surface to volume, have to be considered critically.

Acknowledgement

The authors thank S.W. Sohn for HRTEM investigation and M. Frey for technical support. This work was supported by Leibniz-Institute within the framework “Pakt für Forschung”.

References

[1] R.L. Freed, J.B. Vander Sande, J. Non-Cryst. Solids 27 (1978) 9.
[2] A.J. Kerns, D.E. Polk, R. Ray, B.C. Giessen, Mater. Sci. Eng. 38 (1979) 49.
[3] K.H.J. Buschow, J. Appl. Phys. 52 (1981) 3319.
[4] R.P.W. Lawson, W.A. Grant, P.J. Grundy, Nucl. Instrum. Methods 109 (210;) (1983) 243.
[5] F. Stobiecki, J. Magn. Magn. Mater. 41 (1984) 195.
[6] K.H.J. Buschow, J. Phys. F: Met. Phys. 14 (1984) 593.
[7] Y. Nakagawa, Acta Metall. 6 (1958) 704.
[8] T. Nishizawa, K. Ishida, Bull. Alloy Phase Diagrams 5 (1984) 161.
[9] A. Munitz, S.P. Elder, R. Abbaschian, Metall. Trans. A 23A (1992) 1817.
[10] C.D. Cao, G.P. Görler, D.M. Herlach, B. Wei, Mat. Sci. Eng. A325 (2002) 503.
[11] J.C. Slater, J. Chem. Phys. 41 (1964) 3199.
[12] I.R. Harris, E.M. Carvalho, J. Mater. Sci. 15 (1980) 1224.
[13] A. Dwight, Trans. Am. Inst. Min. Metall. Pet. Eng. 215 (1959) 283.
[14] L. Vegard, Zeit. Phys. 5 (1921) 17.
[15] H.M. Rietveld, J. Appl. Cryst. 2 (1969) 65.
[16] V.I. Nefedov, Y.V. Salyn, A.A. Chertkov, L.N. Padurets, Zh. Neorg. Khim. 19 (1974) 1443.
[17] B. Bondars, G. Heidemane, J. Grabis, K. Laschke, H. Boysen, J. Schneider, F. Frey, J. Mater. Sci. 30 (1995) 1621.
[18] R. Kuentzler, A. Amamou, R. Clad, P. Turek, J. Phys. F: Met. Phys. 17 (1987) 459.
[19] Z. Altounian, J.O. Tu Guo-hua, Strom-Olsen, Solid State Commun. 40 (1981) 221.
[20] T. Saito, IEEE Trans. Mag. 39 (2003) 6044.
[21] T. Saito, Mater. Trans. 44 (2003) 1713.
[22] H. Lu, C.L. Bao, X.N. Yu, Q.K. Xue, D.S. Tang, P.J. Wu, Y.Y. Xiong, Phys. Status Solidi (a) 122 (1990) 481.